

Important Notice to Authors

No further publication processing will occur until we receive your response to this proof.

Attached is a PDF proof of your forthcoming article in *Physical Review Letters*. The article accession code is LS16135. Your paper will be in the following section of the journal: LETTERS — General Physics: Statistical and Quantum Mechanics, Quantum Information, etc.

Please note that as part of the production process, APS converts all articles, regardless of their original source, into standardized XML that in turn is used to create the PDF and online versions of the article as well as to populate third-party systems such as Portico, Crossref, and Web of Science. We share our authors' high expectations for the fidelity of the conversion into XML and for the accuracy and appearance of the final, formatted PDF. This process works exceptionally well for the vast majority of articles; however, please check carefully all key elements of your PDF proof, particularly any equations or tables.

Figures submitted electronically as separate files containing color appear in color in the online journal. However, all figures will appear as grayscale images in the print journal unless the color figure charges have been paid in advance, in accordance with our policy for color in print (<https://journals.aps.org/authors/color-figures-print>).

Specific Questions and Comments to Address for This Paper

The numbered items below correspond to numbers in the margin of the proof pages pinpointing the source of the question and/or comment. The numbers will be removed from the margins prior to publication.

- 1 Please note that PRL journal editor have made slight changes to the title of the letter.
- 2 Please confirm that 78758 is the correct postal code for the fourth affiliation (The University of Texas at Austin).
- 3 The PRL editor has removed the center dot from this expression in accordance with PRL guidelines. See the PRL memo at <https://journals.aps.org/authors/multiplication-signs-h11> for more details concerning this guideline.
- 4 Please define or explain HWP in the Fig. 1 caption.
- 5 Please note that it is journal style to use all capital letters for acronyms generally, and to specifically use IID for independent identically distributed.
- 6 Please review the funding information section of the proof's cover letter and respond as appropriate. We must receive confirmation that the funding agencies have been properly identified before the article can publish.
- 7 NOTE: External links, which appear as blue text in the reference section, are created for any reference where a Digital Object Identifier (DOI) can be found. Please confirm that the links created in this PDF proof, which can be checked by clicking on the blue text, direct the reader to the correct references online. If there is an error, correct the information in the reference or supply the correct DOI for the reference. If no correction can be made or the correct DOI cannot be supplied, the link will be removed.
- 8 Please provide a brief description of the Supplemental Material to be included in Refs. [19, 29, 32] and also note that, URL link will be activated at the time of publication.
- 9 Please provide the name of the city where the publisher is located for Ref. [23].
- 10 A check of online databases revealed a possible error in Ref. [25]. The page number has been changed from "042111" to "16026". Please confirm this is correct.
- 11 Except for the term "and/or," the use of the slash is discouraged between words and abbreviations, as the intent of the solidus is ambiguous. Several possibilities for its meaning exist, among them "and," "or," "and/or," and "plus." We ask that more precise, and therefore more meaningful, conjunctions be used. For terms that are diagrammatically opposed, we use a hyphen (e.g., liquid-solid interface, vacancy-acceptor interface). Please note that input/output was changed to input-output in this reference accordingly.

Titles in References

The editors now encourage insertion of article titles in references to journal articles and e-prints. This format is optional, but if chosen, authors should provide titles for *all* eligible references. If article titles remain missing from eligible references, the production team will remove the existing titles at final proof stage.

Funding Information

Information about an article's funding sources is now submitted to Crossref to help you comply with current or future funding agency mandates. Crossref's Open Funder Registry (<https://www.crossref.org/services/funder-registry/>) is the definitive registry of funding agencies. Please ensure that your acknowledgments include all sources of funding for your article following any requirements of your funding sources. Where possible, please include grant and award ids. Please carefully check the following funder information we have already extracted from your article and ensure its accuracy and completeness:

- Singapore Ministry of Education Academic Research Fund
- National Research Fund
- Ministry of Education - Singapore, FundRef ID <http://dx.doi.org/10.13039/501100001459> (Republic of Singapore/SG)
- Schweizerischer Nationalfonds zur Förderung der Wissenschaftlichen Forschung, FundRef ID <http://dx.doi.org/10.13039/501100001711> (Swiss Confederation/CH)
- Army Research Laboratory Center

Other Items to Check

- Please note that the original manuscript has been converted to XML prior to the creation of the PDF proof, as described above. Please carefully check all key elements of the paper, particularly the equations and tabular data.
- Title: Please check; be mindful that the title may have been changed during the peer-review process.
- Author list: Please make sure all authors are presented, in the appropriate order, and that all names are spelled correctly.
- Please make sure you have inserted a byline footnote containing the email address for the corresponding author, if desired. Please note that this is not inserted automatically by this journal.
- Affiliations: Please check to be sure the institution names are spelled correctly and attributed to the appropriate author(s).
- Receipt date: Please confirm accuracy.
- Acknowledgments: Please be sure to appropriately acknowledge all funding sources.
- References: Please check to ensure that titles are given as appropriate.
- Hyphenation: Please note hyphens may have been inserted in word pairs that function as adjectives when they occur before a noun, as in “x-ray diffraction,” “4-mm-long gas cell,” and “*R*-matrix theory.” However, hyphens are deleted from word pairs when they are not used as adjectives before nouns, as in “emission by x rays,” “was 4 mm in length,” and “the *R* matrix is tested.”
Note also that Physical Review follows U.S. English guidelines in that hyphens are not used after prefixes or before suffixes: superresolution, quasiequilibrium, nanoprecipitates, resonancelike, clockwise.
- Please check that your figures are accurate and sized properly. Make sure all labeling is sufficiently legible. Figure quality in this proof is representative of the quality to be used in the online journal. To achieve manageable file size for online delivery, some compression and downsampling of figures may have occurred. Fine details may have become somewhat fuzzy, especially in color figures. The print journal uses files of higher resolution and therefore details may be sharper in print. Figures to be published in color online will appear in color on these proofs if viewed on a color monitor or printed on a color printer.

- Overall, please proofread the entire *formatted* article very carefully. The redlined PDF should be used as a guide to see changes that were made during copyediting. However, note that some changes to math and/or layout may not be indicated.

Ways to Respond

- **Web:** If you accessed this proof online, follow the instructions on the web page to submit corrections.
- **Email:** Send corrections to aps-robot@luminad.com. Include the accession code LS16135 in the subject line.
- **Fax:** Return this proof with corrections to +1.855.808.3897.

If You Need to Call Us

You may leave a voicemail message at +1.855.808.3897. Please reference the accession code and the first author of your article in your voicemail message. We will respond to you via email.

Randomness Extraction from Bell Violation with Continuous Parametric Down-Conversion

Lijiong Shen,^{1,2} Jianwei Lee,¹ Le Phuc Thinh,¹ Jean-Daniel Bancal,³ Alessandro Cerè,¹ Antia Lamas-Linares,^{4,1}

Adriana Lita,⁵ Thomas Gerrits,⁵ Sae Woo Nam,⁵ Valerio Scarani,^{1,2} and Christian Kurtsiefer^{1,2,*}

¹Centre for Quantum Technologies, National University of Singapore, 3 Science Drive 2, Singapore 117543

²Department of Physics, National University of Singapore, 2 Science Drive 3, Singapore 117551

³Department of Physics, University of Basel, Klingelbergstrasse 82, 4056 Basel, Switzerland

⁴Texas Advanced Computing Center, The University of Texas at Austin, Austin, Texas 78758, USA

⁵National Institute of Standards and Technology, Boulder, Colorado 80305, USA

(Received 8 May 2018)

1 We present a violation of the Clauser-Horne-Shimony-Holt inequality without the fair sampling
2 assumption with a continuously pumped photon pair source combined with two high efficiency
 superconducting detectors. Because of the continuous nature of the source, the choice of the duration of
 each measurement round effectively controls the average number of photon pairs participating in the Bell
 test. We observe a maximum violation of $S = 2.016\,02(32)$ with an average number of pairs per round of
 ≈ 0.32 , compatible with our system overall detection efficiencies. Systems that violate a Bell inequality
 are guaranteed to generate private randomness, with the randomness extraction rate depending on the
 observed violation and on the repetition rate of the Bell test. For our realization, the optimal rate of
 randomness generation is a compromise between the observed violation and the duration of each
 measurement round, with the latter realistically limited by the detection time jitter. Using an extractor
 composable secure against quantum adversary with quantum side information, we calculate an
 asymptotic rate of ≈ 1300 random bits/s. With an experimental run of 43 min, we generated 617 920
 random bits, corresponding to ≈ 240 random bits/s.

DOI:

Based on a violation of a Bell inequality, quantum physics can provide randomness that can be certified to be private, i.e., uncorrelated to any outside process [1–3]. Initial experimental realizations of such sources of certified randomness are based on atomic or atomiclike systems, but exhibit extremely low generation rates, making them impractical for most applications [2,4]. Advances in high efficiency infrared photon detectors [5,6], combined with highly efficient photon pair sources, allowed experimental demonstrations of loophole free violation of the Bell inequality using photons [7–10]. Because of the small observed violation of the Bell inequality in these setups, the random bit generation rate is on the order of tens per second in [11], where they close all loopholes and are limited by the repetition rate of the polarization modulators, and 114 bit/s [12], where they close only the detection loophole and the main limitation is the fixed repetition rate of the photon pair source.

In this work, we use a source of polarization entangled photon pairs operating in a continuous wave (cw) mode, and define measurement rounds by organizing the detection events in uniform time bins. The binning is set independently of the detection time, thus avoiding the coincidence loophole [13,14]. Superconducting detectors with a high detection efficiency allow us to close the

detection loophole. We show how, for fixed overall detection efficiency and pair generation rate, the time bin duration determines the observed Bell violation. We then estimate the rate of random bits that can be extracted from the system and its dependence on time bin width. The simplification of the definition of an experimental round and the absence of an intrinsic dead time found in experiments with pulsed photon pair sources [11,12] lead to a competitive randomness generation rate with a total acquisition time in the order of tens of minutes instead of the tens of hours.

Theory.—Bell tests are carried out in successions of rounds. In each round, each party chooses a measurement and records an outcome. The simplest meaningful scenario involves two parties, each of which can choose between two measurements with binary outcome. Alice and Bob’s measurements are labeled by $x, y \in \{0, 1\}$, respectively; their outcomes are labeled $a, b \in \{+1, -1\}$. As a figure of merit we use the Clauser-Horne-Shimony-Holt (CHSH) expression

$$S = E_{00} + E_{01} + E_{10} - E_{11}, \quad (1)$$

where the correlators are defined by

$$E_{xy} := \Pr(a = b|x, y) - \Pr(a \neq b|x, y). \quad (2)$$

73 As is well known, if $S > 2$, the correlations cannot be due
 74 to preestablished agreement, and if they cannot be attrib-
 75 uted to signaling either, the underlying process is neces-
 76 sarily random. This is not only a qualitative statement: the
 77 amount of extractable private randomness can be quanti-
 78 fied. In the limit in which the statistics are collected from an
 79 arbitrarily large number of rounds, the number of random
 80 bits per round, according to [2], is at least
 81

$$r_\infty \geq 1 - \log_2 \left(1 + \sqrt{2 - \frac{S^2}{4}} \right). \quad (3)$$

82 Tighter bounds on the extractable randomness as a function
 83 of S can be obtained by solving a sequence of semidefinite
 84 programs [2].

85 Besides the no-signaling assumption, this certification of
 86 randomness is device independent: it relies on the value of
 87 S extracted from the observed statistics, but not on any
 88 characterization of the degrees of freedom or of the devices
 89 used in the experiment. All that matters is that in every
 90 round both parties produce an outcome. In our case, we
 91 decide that, if a party's detectors did not fire in a given
 92 round, that party will output $+1$ for that round. This
 93 convention allows us to use only one detector per party
 94 [15,16]: in the rounds when the detector fires, the outcome
 95 will be -1 .

96 While the certification is device independent, the design
 97 of the experiment requires detailed knowledge and control
 98 of the physical degrees of freedom. Our experiment uses
 99 photons entangled in polarization, produced by sponta-
 100 neous parametric down-conversion (SPDC).
 101

102 Let us first consider a simplified model, in which a pair
 103 of photons is created in each round. Eberhard [17] famously
 104 proved that, when the collection efficiencies η_A and η_B
 105 are not unity, higher values of S are obtained using nonmax-
 106 imally entangled pure states. So we aim at preparing

$$|\psi\rangle = \cos\theta|HV\rangle - e^{i\phi}\sin\theta|VH\rangle, \quad (4)$$

107 where H and V represent the horizontal and vertical polari-
 108 zation modes, respectively. The state and measurement that
 109 maximize S are a function of η_A and η_B . For $\phi = 0$, the optimal
 110 measurements correspond to linear polarization directions,
 111 denoted $\cos\alpha_x\hat{e}_H + \sin\alpha_x\hat{e}_V$ and $\cos\beta_y\hat{e}_H + \sin\beta_y\hat{e}_V$.

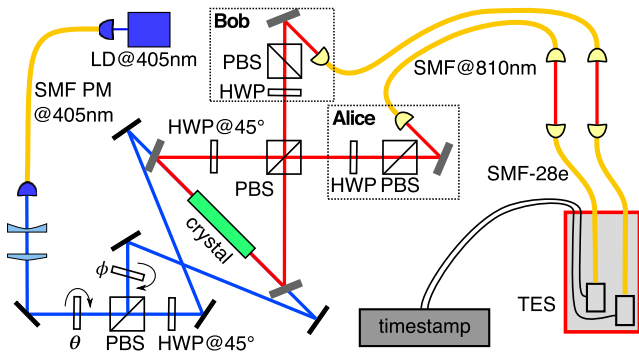
112 For a down-conversion source, the number of photons
 113 produced per round is not fixed. If the duration τ of a round
 114 is much longer than the single-photon coherence time, and
 115 no multiphoton states are generated (a realistic assumption
 116 in a cw pumped scenario), the output of the source is
 117 accurately described by independent photon pairs, whose
 118 number v follows a Poissonian distribution $P_\mu(v)$ of
 119 average pairs per round μ . The main contribution to $S >$
 120 2 will come from the single-pair events; notice that $P_\mu(1) \leq$
 121 $(1/e) \approx 0.37$ for a Poissonian distribution. So there is
 122 always a large fraction of other pair number events, and
 123

the observed value of S depends significantly on it [18].
 For $\mu \rightarrow 0$, almost all rounds will give no detection, that is
 $P(+1, +1|x, y) \approx 1$, which leads to $S = 2$. So, for $\mu \ll 1$
 we expect a violation $S \approx P_\mu(1)S_{\text{qubits}} + [1 - P_\mu(1)]2$,
 where S_{qubits} is the value achievable with state (4). In the
 other limit, $\mu \gg 1$, almost all rounds will have a detection,
 that is, $P(-1, -1|x, y) \approx 1$ and again $S = 2$. Before this
 behavior kicks in, when more than one pair is frequently
 present we expect a drop in the value of S , since the detections
 may be triggered by independent pairs. An accurate model-
 ing for any value of μ is conceptually simple but notationally
 cumbersome (see Supplemental Material [19]).

Photon pair sources based on pulsing quasi-cw sources
 with a fixed repetition rate control the value of μ by limiting
 the pump power. With true cw pumping the average
 number of pairs per round is $\mu = (\text{pair rate})\tau$, where τ is
 the round duration. The resulting repetition rate of the
 experiment is $1/\tau$. In this work, we fix the pair rate, while τ
 is a free parameter that can be optimized to extract the
 highest amount of randomness.

Experimental setup.—A sketch of the experimental
 setup is shown in Fig. 1. The source for entangled photon
 pairs is based on the coherent combination of two
 collinear type-II SPDC processes [20]. We pump a
 periodically poled potassium titanyl phosphate crystal
 (PPKTP, $2 \times 1 \times 10 \text{ mm}^3$) from two opposite directions
 with light from the same laser diode (405 nm). Both pump
 beams have the same Gaussian waists of $\approx 350 \mu\text{m}$ located
 within the crystal. Light at 810 nm from the two SPDC
 processes is overlapped in a polarizing beam splitter
 (PBS), entangling the polarization modes, and collected
 into single mode fibers. When a single-photon pair is
 generated, the resulting polarization state is given by
 Eq. (4), where θ and ϕ are determined by the relative
 intensity and phase of the two pump beams set by rotating
 a half-wave plate before the first PBS, and the tilt of a
 glass plate in one of the pump arms.

The effective collection modes for the down-converted
 light, determined by the single mode optical fibers and
 incoupling optics was chosen to have a Gaussian beam
 waist of $\approx 130 \mu\text{m}$ centered in the crystal in order to
 maximize collection efficiency [21,22]. The combination
 of a zero-order half-wave plate and another PBS (extinction
 rate 1:1000 in transmission) sets the measurement bases
 for light entering the single mode fibers. All optical
 elements are antireflection coated for 810 nm. Light from
 each collection fiber is sent to a superconducting transition
 edge sensor (TES) optimized for detection at 810 nm [5],
 which are kept at $\approx 80 \text{ mK}$ within a cryostat. As the
 detectors show the highest efficiency when coupled to
 telecom fibers (SMF28+), the light collected in to single
 mode fibers from the parametric conversion source is
 transferred to these fibers via a free-space link. The TES
 output signal is translated into photodetection event arrival
 times using a constant fraction discriminator with an overall



F1:1 FIG. 1. Schematic of the experimental setup, including the
 F1:2 source of the nonmaximally entangled photon pairs. A PPKTP
 F1:3 crystal, cut and poled for type II spontaneous parametric down-
 F1:4 conversion from 405 to 810 nm, is placed at the waist of a
 F1:5 Sagnac-style interferometer and pumped from both sides. Light
 F1:6 at 810 nm from the two SPDC process is overlapped in a polarizing
 F1:7 beam splitter (PBS), generating the nonmaximally entangled state
 F1:8 described by Eq. (4) when considering a single photon pair. A
 F1:9 laser diode (LD) provides the continuous wave UV pump light.
 F1:10 The combination of a half-wave plate and polarization beam
 F1:11 splitter (PBS) sets θ by controlling the relative intensity of the two
 F1:12 pump beams, while a thin glass plate controls their relative phase
 F1:13 ϕ . The pump beams enter the interferometer through dichroic
 F1:14 mirrors. At each output of the PBS, the combination of a HWP
 F1:15 and PBS projects the mode polarization before coupling into a
 F1:16 fiber single mode for light at 810 nm (SMF@810). A free-space
 F1:17 link is used to transfer light from SMF@810 to single mode fibers
 F1:18 designed for 1550 nm (SMF-28e). Eventually, the light is
 F1:19 detected with high efficiency superconducting transition edge
 F1:20 sensors (TES), and time stamped with a resolution of 2 ns.

179 timing jitter ≈ 170 ns, and recorded with a resolution of
 180 2 ns. Setting Alice's and Bob's analyzing wave plates in the
 181 natural basis of the combining PBS, HV and VH , we
 182 estimate heralded efficiencies of $82.42 \pm 0.31\%$ (HV) and
 183 $82.24 \pm 0.30\%$ (VH). We identified two main sources of
 184 uncorrelated detection events: intrinsic detector and back-
 185 ground events at rates of 6.7 ± 0.58 s^{-1} for Alice and
 186 11.9 ± 0.77 s^{-1} for Bob, respectively, and fluorescence
 187 caused by the UV pump in the PPKTP crystal [23],
 188 contributing $0.135 \pm 0.08\%$ of the signal. With a total
 189 pump power at the crystal of 5.8 mW we estimate a pair
 190 generation rate $\approx 2.4 \times 10^4$ s^{-1} (detected $\approx 20 \times 10^3$ s^{-1}),
 191 and dark count-background rates of 45.7 s^{-1} (Alice) and
 192 41.5 s^{-1} (Bob).

193 *Violation.*—For the measured system efficiencies ($\eta_A \approx$
 194 82.4% , $\eta_B \approx 82.2\%$) and rate of uncorrelated counts at
 195 each detector (45.7 s^{-1} Alice, 41.5 s^{-1} Bob), a numerical
 196 optimization gives the following values of the state and
 197 measurement parameters (see [19] for details): $\theta = 25.9^\circ$,
 198 $\alpha_0 = -7.2^\circ$, $\alpha_1 = 28.7^\circ$, $\beta_0 = 82.7^\circ$, and $\beta_1 = -61.5^\circ$.
 199 These are close to optimal for all values of μ , and the
 200 maximal violation is expected for $\mu = 0.322$.

201 We collected data for approximately 42.8 min, changing
 202 the measurement basis every 2 min, cycling through the

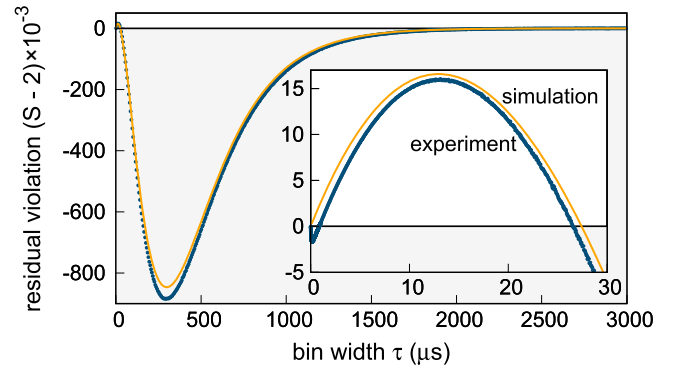
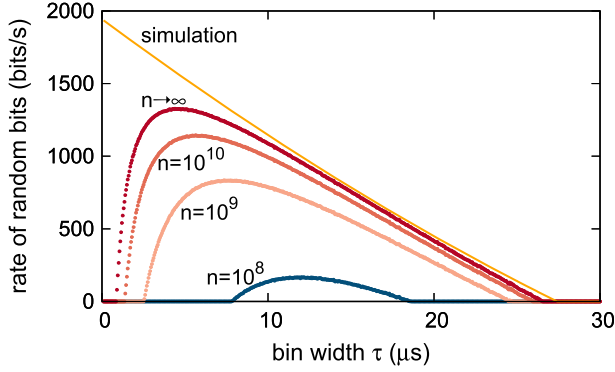


FIG. 2. Measured CHSH violation as a function of bin width τ
 (blue circles). A theoretical model (orange continuous line) is
 sketched in the main text and described in detail in [19]. Both
 the simulation and the experimental data show a violation for short
 τ (zoom in inset). The uncertainty on the measured value, calcu-
 lated assuming IID, corresponding to one standard deviation due
 to a Poissonian distribution of the events, is smaller than the
 symbols. For $\tau \lesssim 1$ μs the detection jitter (≈ 170 ns) is com-
 parable with the time bin, resulting in a loss of observable
 correlation and a fast drop of the value of S .

four possible basis combinations. The sequence of the four
 settings is determined for every cycle using a pseudoran-
 dom number generator. We periodically ensure that $\phi \approx 0$
 by rotating the phase plate until the visibility in the
 $+45^\circ/-45^\circ$ basis is larger than 0.985. Excluding the
 phase lock, the effective data acquisition time is ≈ 34 min.

In Fig. 2 we show the result of processing the time
 stamped events for different bin widths τ . The largest
 violation $S = 2.01602(32)$ is observed for $\tau = 13.150$ μs ,
 which, with the cited pair generation rate of 24×10^3 s^{-1} ,
 corresponds to $\mu \approx 0.32$. The uncertainty is calculated
 assuming that measurement results are independent and
 identically distributed (IID). Since the fluctuations of S are
 identical in the IID and non-IID settings, this uncertainty is
 also representative of the p value associated with local
 models [24,25]. The slight discrepancy between the exper-
 imental violation and the simulation is attributed to the
 nonideal visibility of the state generated by the photon
 pair source. When τ is comparable to the detection jitter,
 detection events due to a single pair may be assigned
 to different rounds, decreasing the correlations. This
 explains the drop of S below 2 (which our simulation
 does not capture because we have not included the jitter as
 a parameter).

Randomness extraction.—In order to turn the output
 data generated from our experiment into uniformly ran-
 dom bits, we need to employ a randomness expansion
 protocol [26]. Such a protocol consists of a predefined
 number of rounds n , forming a block. Each round is
 randomly assigned (with probability γ and $1 - \gamma$, respec-
 tively) to one of two tasks: testing the device for faults or
 eavesdropping attempts, or generating random bits. When
 the test rounds show a sufficient violation, one applies a



F3:1 FIG. 3. Randomness generation rate r_n/τ as a function of τ
 F3:2 for different block sizes n . The points are calculated via Eq. (5)
 F3:3 for finite n [Eq. (6) for $n \rightarrow \infty$] and the violation measured in
 F3:4 the experiment, assuming $\gamma = 0$ (no testing rounds) and $\epsilon_c =$
 F3:5 $\epsilon_s = 10^{-10}$. The continuous line is the asymptotic rate Eq. (6)
 F3:6 evaluated on the values of S of the simulation shown in Fig. 2,
 F3:7 for the same security assumptions.

236 quantum-proof randomness extractor to the block, obtaining
 237 m random bits. The performance of the extraction protocol
 238 [27] is determined by completeness and soundness security
 239 parameters ϵ_c and ϵ_s . To ensure the resulting string is
 240 uniform to within $\approx 10^{-10}$, we choose $\epsilon_c = \epsilon_s = 10^{-10}$.
 241 The extraction protocol is a one-shot extraction protocol;
 242 i.e., the security analysis does not assume IID. The output
 243 randomness is composable and secure against a quantum
 244 adversary holding quantum side information [26]. The
 245 details of the protocol execution (using also [28]) and its
 246 security proof are given in [29].

247 For a block consisting of n rounds, the number of
 248 random bits per round is at least

$$r_n = \eta_{\text{opt}}(\epsilon', \epsilon_{\text{EA}}) - 4 \frac{\log n}{n} + 4 \frac{\log \epsilon_{\text{EX}}}{n} - \frac{10}{n}, \quad (5)$$

249 where the function η_{opt} depends on the block size n ,
 250 detected violation S , and auxiliary security parameters ϵ' ,
 251 ϵ_{EA} , ϵ_{EX} . The choice of these auxiliary security parameters
 252 is required to add up to the chosen level of completeness
 253 and soundness. In the limit $n \rightarrow \infty$ we obtain a lower
 254 bound on the number of random bits per round
 255

$$r_\infty = 1 - h\left(\frac{1}{2} + \frac{1}{2}\sqrt{\frac{S^2}{4} - 1}\right), \quad (6)$$

256 where $h(p) := -p \log_2 p - (1-p) \log_2(1-p)$ is the
 257 binary entropy function.

259 The extractable randomness rate r_n/τ based on the
 260 observed S is presented in Fig. 3 for various block sizes
 261 n . For comparison, we also plot the asymptotic value r_∞/τ
 262 with S given by the simulation. The most obvious feature
 263 is that the highest randomness rate is not obtained at
 264 maximal violation of the inequality. There, one gets highest

265 randomness per round, but it turns out to be advantageous
 266 to sacrifice randomness per round in favor of a larger
 267 number of rounds per unit time. This optimization will be
 268 part of the calibration procedure for a random number
 269 generator with an active switch of measurement bases. As
 270 explained previously, the detection jitter affects the observ-
 271 able violation for τ comparable to it. This causes the sharp
 272 drop for short time bins observed for the experimental data.
 273 For fixed detector efficiencies, we expect the randomness
 274 rate to increase with higher photon pair generation rate, that
 275 is by increasing the pump power, and to be ultimately
 276 limited by the detection time jitter. Here, the use of efficient
 277 superconducting nanowire detectors will be a significant
 278 advantage.

279 We generated a random string from the data used to
 280 demonstrate the violation. We sacrificed $\approx 22\%$ of the data
 281 as calibration to determine the optimal bin width ($8.9 \mu\text{s}$),
 282 and estimate the corresponding violation. We applied the
 283 extractor to the remaining $\approx 78\%$ of the data, corresponding
 284 to 175 288 156 bins, obtaining 617 920 random bits,
 285 passing the NIST test suite [30]. The extractor required
 286 a seed provided by the random number generator in [31].
 287 From the total measurement time of 42.8 min, we calculate
 288 a rate of ≈ 240 random bit/s. For details of the extraction
 289 process see [32]. Considering only the net measurement
 290 time, that is without the acquisition of the calibration
 291 fraction of the data, the phase lock of the source, and
 292 the rotation of wave plate motors, we obtain a randomness
 293 rate of ≈ 396 bit/s. These numbers are not necessarily
 294 optimal; more sophisticated analysis demonstrated randomness
 295 extraction for very low detected violations [11,33],
 296 and may yield a larger extractable randomness also in our
 297 case. Details of the extraction procedure are in [32].

298 *Conclusion.*—We experimentally observed a violation of
 299 CHSH inequality with a continuous wave photon entangled
 300 pair source without the fair-sampling assumption combin-
 301 ing a high collection efficiency source and high detection
 302 efficiency superconducting detectors, with the largest
 303 detected violation of $S = 2.016\,02(32)$.

304 The generation rate of all probabilistic sources of
 305 entangled photon pairs is limited by the probability of
 306 generation of multiple pairs per experimental round,
 307 according to Poissonian statistics. The flexible definition
 308 of an experimental round permitted by the cw nature of our
 309 setup allowed us to study the dependence of the observable
 310 violation as function of the average number of photon
 311 pairs per experimental round. This same flexibility can be
 312 exploited to reduce the time necessary to acquire sufficient
 313 statistics for these kinds of experiments: an increase in the
 314 pair generation rate is accompanied by a reduction of the
 315 round duration. This approach shifts the experimental
 316 repetition rate limitation from the photon statistics to the
 317 other elements of the setup, e.g., detectors time response or
 318 active polarization basis switching speed.

319 The observation of a Bell violation also certifies the
 320 generation of randomness. We estimate the amount of

321 randomness generated per round both in an asymptotic
 322 regime and for a finite number of experimental rounds,
 323 assuming a required level of uniformity of 10^{-10} . When
 324 considering the largest attainable *rate* of random bit
 325 generation, the optimal round duration is the result of
 326 the trade-off between observed violation and the number of
 327 rounds per unit time. While for an ideal realization the
 328 optimal round duration would be infinitesimally short, it is
 329 limited in our system by the detection jitter time. Our proof
 330 of principle demonstration can be extended into a complete,
 331 loophole-free random number source. This requires closing
 332 the locality and freedom-of-choice loopholes, with techni-
 333 ques not different from pulsed photonic sources, with the
 334 only addition of a periodic calibration necessary for
 335 determining the optimal time bin.

336 **6** This research is supported by the Singapore Ministry of
 337 Education Academic Research Fund Tier 3 (Grant
 338 No. MOE2012-T3-1-009); by the National Research
 339 Fund and the Ministry of Education, Singapore, under
 340 the Research Centres of Excellence programme; by the
 341 Swiss National Science Foundation (SNSF), through
 342 Grants No. PP00P2-150579 and No. PP00P2-179109;
 343 and by the Army Research Laboratory Center for
 344 Distributed Quantum Information via the project SciNet.

345 Contributions to this Letter by workers at NIST, an
 346 agency of the U.S. Government, are not subject to U.S.
 347 copyright.

350
 348
 351 *christian.kurtsiefer@gmail.com

352 **7** [1] R. Colbeck, Ph.D. thesis, University of Cambridge, 2007.
 353 [2] S. Pironio, A. Acín, S. Massar, A. B. de la Giroday, D. N.
 354 Matsukevich, P. Maunz, S. Olmschenk, D. Hayes, L. Luo,
 355 T. A. Manning, and C. R. Monroe, *Nature (London)* **464**,
 356 **1021** (2010).
 357 [3] A. Acín and L. Masanes, *Nature (London)* **540**, 213 (2016).
 358 [4] B. J. Hensen, H. Bernien, A. E. Dréau, A. Reiserer, N. Kalb,
 359 M. S. Blok, J. Ruitenberg, R. F. L. Vermeulen, R. N.
 360 Schouten, C. Abellán, W. Amaya, V. Pruneri, M. W.
 361 Mitchell, M. Markham, D. J. Twitchen, D. Elkouss, S.
 362 Wehner, T. H. Taminiau, and R. Hanson, *Nature (London)*
 363 **526**, 682 (2015).
 364 [5] A. E. Lita, A. J. Miller, and S. W. Nam, *Opt. Express* **16**,
 365 **3032** (2008).
 366 [6] F. Marsili, V. B. Verma, J. A. Stern, S. Harrington, A. E.
 367 Lita, T. Gerrits, I. Vayshenker, B. Baek, M. D. Shaw, R. P.
 368 Mirin, and S. W. Nam, *Nat. Photonics* **7**, 210 (2013).
 369 [7] M. Genovese, *Phys. Rep.* **413**, 319 (2005).
 370 [8] N. Brunner, D. Cavalcanti, S. Pironio, V. Scarani, and S.
 371 Wehner, *Rev. Mod. Phys.* **86**, 419 (2014).
 372 [9] M. Giustina, M. A. M. Versteegh, S. Wengerowsky, J.
 373 Handsteiner, A. Hochrainer, K. Phelan, F. Steinlechner, J.
 374 Kofler, J.-A. Larsson, C. Abellán, W. Amaya, V. Pruneri,
 375 M. W. Mitchell, J. Beyer, T. Gerrits, A. E. Lita, L. K. Shalm,
 376 S. W. Nam, T. Scheidl, R. Ursin, B. Wittmann, and A.
 377 Zeilinger, *Phys. Rev. Lett.* **115**, 250401 (2015).

[10] L. K. Shalm, E. Meyer-Scott, B. G. Christensen, and P. 378
 Bierhorst, *Phys. Rev.* **115**, 250402 (2015). 379
 [11] P. Bierhorst, E. Knill, S. Glancy, Y. Zhang, A. Mink, S. Jordan, 380
 A. Rommal, Y.-K. Liu, B. Christensen, S. W. Nam, M. J. 381
 Stevens, and L. K. Shalm, *Nature (London)* **556**, 223 (2018). 382
 [12] Y. Liu, X. Yuan, M.-H. Li, W. Zhang, Q. Zhao, J. Zhong, Y. 383
 Cao, Y.-H. Li, L.-K. Chen, H. Li, T. Peng, Y.-A. Chen, C.-Z. 384
 Peng, S.-C. Shi, Z. Wang, L. You, X. Ma, J. Fan, Q. Zhang, 385
 and J.-W. Pan, *Phys. Rev. Lett.* **120**, 010503 (2018). 386
 [13] J.-A. Larsson and R. D. Gill, *Europhys. Lett.* **67**, 707 (2004). 387
 [14] B. G. Christensen, A. Hill, P. G. Kwiat, E. Knill, S. W. Nam, 388
 K. Coakley, S. Glancy, L. K. Shalm, and Y. Zhang, *Phys.* 389
Rev. A **92**, 032130 (2015). 390
 [15] M. Giustina, A. Mech, S. Ramelow, B. Wittmann, J. Kofler, 391
 J. Beyer, A. E. Lita, B. Calkins, T. Gerrits, S. W. Nam, R. 392
 Ursin, and A. Zeilinger, *Nature (London)* **497**, 227 (2013). 393
 [16] J.-D. Bancal, L. Sheridan, and V. Scarani, *New J. Phys.* **16**, 394
033011 (2014). 395
 [17] P. H. Eberhard, *Phys. Rev. A* **47**, R747 (1993). 396
 [18] V. Caprara Vivoli, P. Sekatski, J.-D. Bancal, C. C. W. Lim, 397
 B. G. Christensen, A. Martin, R. T. Thew, H. Zbinden, N. 398
 Gisin, and N. Sangouard, *Phys. Rev. A* **91**, 012107 (2015). 399
 [19] See Supplemental Material, part A, at [http://link.aps.org/](http://link.aps.org/supplemental/10.1103/PhysRevLett.000.000000) **8** 400
[supplemental/10.1103/PhysRevLett.000.000000](http://link.aps.org/supplemental/10.1103/PhysRevLett.000.000000) for model- 401
 ing the violation of CHSH by a Poissonian source of qubit 402
 pairs. 403
 [20] M. Fiorentino, G. Messin, C. E. Kuklewicz, F. N. C. Wong, 404
 and J. H. Shapiro, *Phys. Rev. A* **69**, 041801 (2004). 405
 [21] R. S. Bennink, *Phys. Rev. A* **81**, 053805 (2010). 406
 [22] P. B. Dixon, D. Rosenberg, V. Stelmakh, M. E. Grein, R. S. 407
 Bennink, E. A. Dauler, A. J. Kerman, R. J. Molnar, and 408
 F. N. C. Wong, *Phys. Rev. A* **90**, 043804 (2014). 409
 [23] S. M. Hegde, K. L. Schepler, R. D. Peterson, and D. E. 410
 Selmon, in *Defense and Security Symposium*, edited by 411
 G. L. Wood and M. A. Dubinskii (SPIE, 2007), p. 65520V. **9** 412
 [24] P. Bierhorst, *J. Phys. A* **48**, 195302 (2015). 413
 [25] D. Elkouss and S. Wehner, *npj Quantum Inf.* **2**, 16026 **10** 414
(2016). 415
 [26] R. Arnon-Friedman, F. Dupuis, O. Fawzi, R. Renner, and T. 416
 Vidick, *Nat. Commun.* **9**, 459 (2018). 417
 [27] W. Mauerer, C. Portmann, and V. B. Scholz, [arXiv:1212](https://arxiv.org/abs/1212.0520) 418
.0520. 419
 [28] T. S. Hao and M. Hoshi, *IEEE Trans. Inf. Theory* **43**, 599 420
(1997). 421
 [29] See Supplemental Material, part B, at [http://link.aps.org/](http://link.aps.org/supplemental/10.1103/PhysRevLett.000.000000) 422
[supplemental/10.1103/PhysRevLett.000.000000](http://link.aps.org/supplemental/10.1103/PhysRevLett.000.000000) for the de- 423
 tails of the protocol and a security proof, and part C for an 424
 input-output randomness analysis. **11** 425
 [30] A. Rukhin, J. Soto, J. Nechvatal, M. Smid, E. Barker, S. 426
 Leigh, M. Levenson, M. Vangel, D. Banks, A. Heckert, J. 427
 Dray, and S. Vo, *A Statistical Test Suite for the Validation of* 428
Cryptographic Random Number Generators (National In- 429
 stitute of Standards and Technology, Gaithersburg, MD, 430
 2010). 431
 [31] Y. Shi, B. Chng, and C. Kurtsiefer, *Appl. Phys. Lett.* **109**, 432
041101 (2016). 433
 [32] See Supplemental Material, part D, at [http://link.aps.org/](http://link.aps.org/supplemental/10.1103/PhysRevLett.000.000000) 434
[supplemental/10.1103/PhysRevLett.000.000000](http://link.aps.org/supplemental/10.1103/PhysRevLett.000.000000) for the 435
 random bit extraction procedure. 436
 [33] E. Knill, Y. Zhang, and P. Bierhorst, [arXiv:1709.06159](https://arxiv.org/abs/1709.06159). 437
 438